

Decitabine induces change of biological traits in myelodysplastic syndromes via FOXO1 activation

Zheng Zhang

Department of Hematology, Shanghai Jiao Tong University Affiliated Sixth People's Hospital, Shanghai, China

Yan Jia

Department of Hematology, Shanghai Jiao Tong University Affiliated Sixth People's Hospital, Shanghai, China

Feng Xv

Department of Hematology, Shanghai Jiao Tong University Affiliated Sixth People's Hospital, Shanghai, China

Lu-xi Song

Department of Hematology, Shanghai Jiao Tong University Affiliated Sixth People's Hospital, Shanghai, China

Lei Shi

Department of Hematology, Shanghai Jiao Tong University Affiliated Sixth People's Hospital, Shanghai, China

Juan Guo

Department of Hematology, Shanghai Jiao Tong University Affiliated Sixth People's Hospital, Shanghai, China

Chunkang Chang (✉ changchunkang@sjtu.edu.cn)

Shanghai Jiao Tong University Affiliated Sixth People's Hospital

Research

Keywords: Myelodysplastic syndromes, DEGs, FOXO1, PTEN, TLR4

Posted Date: August 1st, 2020

DOI: <https://doi.org/10.21203/rs.3.rs-48006/v1>

License:  This work is licensed under a Creative Commons Attribution 4.0 International License.

[Read Full License](#)

Version of Record: A version of this preprint was published at Frontiers in Genetics on January 27th, 2021. See the published version at <https://doi.org/10.3389/fgene.2020.603956>.

Abstract

Background: Little is known about the function of tumor suppressor gene Forkhead box 1 (FOXO1) in myelodysplastic syndromes (MDS). The aim of this study was to elucidate the role of FOXO1 through decitabine (DAC) treatment.

Methods: Microarray analysis was used to identify differentially expressed genes (DEGs) from 2 MDS cell lines by DAC treatment. WebGestalt was used to perform gene ontology (GO), Kyoto Encyclopedia of Genes and Genomes (KEGG) pathway enrichment analysis, and STRING (Search Tool for the Retrieval of Interacting Genes/Proteins) for constructing protein–protein interaction (PPI) network analysis. Cell apoptosis, cycle arrest, differentiation, and immunoregulation were performed to validate the function of FOXO1 by silencing its expression prior to DAC treatment in MDS.

Results: The results showed that the FOXO signaling pathway was one of the most promising. FOXO1 exists in a hyperphosphorylated, inactive form in MDS-L cells. DAC treatment both induces FOXO1 expression and reactivates the protein through reducing its phosphorylation level. Furthermore, we showed that this FOXO1 activation is responsible for the DAC-induced apoptosis, cell cycle arrest, antigen differentiation, and immunoregulation in MDS-L cells. The results also demonstrated that DAC-induced FOXO1 activation upregulated anti-tumor immune response in higher risk MDS specimens.

Conclusions: These results suggest that DAC induces FOXO1 activation, which plays an important role in anti-MDS tumors.

Background

Myelodysplastic syndrome (MDS) is a group of highly heterogeneous myeloid neoplasms, characterized by inefficient hematopoiesis, variable cytopenias and a considerable risk of progression to acute myeloid leukemia. The incidence of MDS in the elderly gradually increases with age, which is one of the main factors that threaten the quality of life and survival of the elderly. Although 3 therapies targeting MDS have been approved since 2004, the overall 5-year survival rate remains relatively poor at approximately 31% without a clear temporal improvement in outcomes [1]. The heterogeneous nature of MDS demands a complex and personalized variety of therapeutic approaches. Accurate determination of prognosis is critical to select an appropriate therapy and to predict the prognosis of patients with MDS. According to the International Prognostic Scoring System (IPSS) or revised IPSS (IPSS-R), approximately 30% of patients are categorized as higher-risk groups [2, 3]. Hypomethylating agents (HMAs), such as decitabine (DAC), are approved as the first-line treatment option for higher- risk MDS. DAC has a wide range of therapeutic mechanisms for MDS, which reactivates silenced tumor suppressor genes, increases expression of cancer-testis antigens (CTAs), and regulates immune checkpoint molecules [4–6]. Previous studies have shown that epigenetic silencing of tumor suppressor genes results in the growth advantage of a clonal subpopulation of MDS. This epigenetic modification is reversible, and methyltransferase inhibitors, such as DAC, will reverse the situation and reactivate the silenced tumor suppressor genes [7].

The “O” subclass of the forkhead transcription factors (FOX) family is considered important tumor suppressor genes, which are found in a broad range of living organisms, playing an important role in the longevity of invertebrates and mammals, and they suppress tumor proliferation and regulate of energy metabolism and the induction of cellular response [8]. In fact, a study has investigated the effects of DAC treatment on the myeloid MDS cell line SKM-1 and investigated the role of FOXO3A in DAC-dependent treatment [9]. Currently, no studies have investigated the pathogenesis of FOXO1 in MDS.

FOXO1, also known as forkhead in rhabdomyosarcoma-like protein 1 (FKHRL1), is another key transcription factor of the FOX family with important roles in apoptosis, autophagy, anti-oxidative enzymes, cell cycle arrest, and metabolic and immune regulators, rendering it a super transcription factor with complex activities [10, 11]. It is characterized by the presence of the distinctive forkhead DNA binding domain, a highly conserved winged helix motif, and regulates the transcription of a variety of downstream genes [12]. The function of FOXO1 is not only regulated by microRNAs, which play important roles in destabilizing or attenuating the translation of FOXO1 mRNA, but also by post-translational modifications (such as phosphorylation, acetylation, and ubiquitination), which ultimately affect its nuclear/cytoplasmic transport and thus its cellular localization [13]. After FOXO1 is phosphorylated, p-FOXO1 binds to the cytoplasm by 14-3-3 proteins and is involved in the subsequent interaction with ubiquitin E3 ligases, which induces its degradation, FOXO1 is inactivated and its target gene is down-regulated [14]. Furthermore, FOXO1 is directly or indirectly regulated by other protein kinases (such as AKT, MAPK1 and PTEN). FOXO1 is considered as a potential tumor suppressor gene that participates in the regulation of the differentiation of a variety of cells and plays a role in inhibiting tumor cell proliferation [15]. An increasing number of studies have confirmed that the re-expression and activation of FOXO1 in tumor cells has great potential in anti-tumor therapy [16].

In this study, we investigated the effects of a low concentration of DAC (1 μ M) on differentially expressed genes (DEGs), cell apoptosis, cycle arrest, differentiation, and immunoregulation in MDS cell lines and patients. In addition, we also investigated the role of FOXO1 in DAC-dependent processes by measuring the expression level and activity of this gene and its downstream targets after DAC treatment.

Methods

Cell Culture and DAC Treatment

MDS-L cells were donated by Prof. Tohyama [17]. MDS-derived leukemia cell line SKM-1 cells were donated by Prof. Nakagawa [18]. Cell lines were cultured in RPMI 1640 containing 10% heat-inactivated fetal bovine serum and 1% penicillin-streptomycin at 37 °C in a humidified atmosphere containing 5% CO₂. In addition, IL-3 (100 U/ml) is essential for MDS-L cells. When cells reached the logarithmic growth phase, they were seeded at a density of 5×10^5 cells/ well in 6-well plates and treated with five 24-h pulses of 1 μ M DAC (Selleck Chemicals LLC, Houston TX, USA) and harvested after the treatment.

RNA Preparation and Gene Expression Microarray (GEM)

As previously described [19], total RNA was extracted from 10^5 cell lines using the RNeasy system (Qiagen, Valencia, CA) following the manufacturer's instructions. A Genechip Primeview™ Human Gene Expression Array (Affymetrix, US) was used for the GEM study. The signal intensities were acquired with a Genechip Scanner 3000 7G (Affymetrix) to generate cell intensity files (CEL). The statistical analysis was performed using the Partek Genomics Suite software (Partek, Inc., St. Louis, MO, USA). A robust multi-array average (RMA) algorithm was used to normalize the data. The false discovery rate (FDR) was less than 0.15 to minimize the false identification of genes. Changes greater than 1.0-fold were analyzed for up- or downregulated genes.

Functional Enrichment Analysis

WebGestalt (<http://www.webgestalt.org/option.php>) is an automated systematic-analysis tool that helps understand common and unique way within a set of orthogonal target discovery researches. The tool is free and well-maintained, user-friendly gene-list analysis for gene annotation and analysis. The gene ontology (GO) terms for biological process (BP), cellular component (CC), and molecular function (CC) categories, as well as Kyoto Encyclopedia of Genes and Genomes (KEGG) pathways was performed using the WebGestalt online tool. GraphPad (GraphPad Software, Inc., San Diego, CA, USA) was used to improve GO graphic analysis. Fisher's exact test was used to select the significant pathway, and the threshold of significance was defined by FDR. P-value < 0.05 was considered statistically significant. STRING (<http://string-db.org>) was used to construct protein–protein interaction (PPI) network of DEGs for DAC treatment MDS cell lines and the confidence score of the interaction > 0.4 was considered statistically significant. Cytoscape was employed to annotate and improve the up-down regulated genes of PPI. Further, molecular complex detection (MCODE) APP was applied to identify densely connected network components.

Cellular Transfection

MDS-L cells were transfected with either Silencer Select FOXO1 (cat. AM16708) or Silencer Select Negative Control (cat. AM4611) siRNAs, both of which were purchased from Thermo Fisher (Thermo Fisher Scientific, Waltham, MA, USA), and Lipofectamine 3000 reagent (Thermo Fisher Scientific, Waltham, MA) according to previously reported literature [9]. The harvest time of these transfected cells was set to 24 h post-transfection. Then, the transfected cells were either cultured or treated with 1 μ M of DAC for 72 hours as required.

Apoptosis assessment

Cell apoptosis analysis was fulfilled by employing an annexin V-FITC/PI apoptosis detection kit (BD Biosciences) with a flow cytometer (FACS Calibur, BD Biosciences, Franklin Lakes, NJ, USA). MDS-L cells were inoculated in 6-well plates at the density of 10^5 cells each well following different experimental manipulation. Subsequently, these cells were first suspended in binding buffer, and then Annexin V-FITC (10 μ l) and PI (5 μ l) were respectively supplied to each well. Finally, flow cytometry (FCM) analysis was performed after the mixtures reacted in dark condition for 15 min.

Cell cycle analysis

5×10^4 cells were washed with cold phosphate-buffered saline (PBS), fixed in 70% ethanol, washed with PBS once more, and then re-suspended in 1 mL of propidium iodide (PI) staining reagent (50 mg/ml of propidium iodide and 1 mg/ml of RNase). Samples were incubated in the dark for 30 min before cell cycle analysis. The cell cycle was measured with FACS Calibur. The percentages of cells in the G1, S, and G2 phases were calculated with the Cellquest software.

Detection of Cell Surface Markers

DAC-treated MDS-L cells were collected and stained for surface antigen, 10 μ l of PerCP-bound anti-CD3 antibody, APC-bound anti-CD13 antibody, FITC-bound anti-CD14 antibody, PE-bound anti-CD20 antibody or PE-bound anti-235a antibody (Becton Dickinson) was added to the cells and incubated for 15 minutes at room temperature in the darkness. Cells were then washed and resuspended in PBS, and surface markers were analyzed by FCM within 1 h.

Bone marrow mononuclear cells and T lymphocytes preparation

Twelve MDS patients were administered with DAC (product name: Dacogen, DAC, Xian Janssen Pharmaceutical Ltd., 20 mg/M² \times 5 d for 4 courses) for immune research after obtaining informed consent in accordance with the Declaration of Helsinki. MDS were diagnosed according to the World Health Organization (WHO) 2016 criteria [20], and the detailed information regarding MDS patients is shown in Supplementary Table 1. Five milliliters of fresh bone marrow was aspirated from posterior iliac crests. Bone marrow mononuclear cells (BM-MNCs) were isolated using Ficoll-Hypaque gradient (Lymphoprep TM, Niergaard, Oslo, Norway) for mRNA expression by quantitative real-time polymerase chain reaction (PCR). BM-MNCs of some MDS patients were carefully separated into 2 portions, T cells of 1 part were isolated using MACS CD3 + T microbeads (Miltenyi Biotec), followed by RT² Profiler PCR Arrays and the rest of the BM-MNCs were used for western blot analysis.

Western blot analysis

Whole cell lysates were obtained from MDS-L cell line or BM-MNCs of MDS patients, and equal quantities of protein were separated by 12% sodium dodecyl sulfate polyacrylamide gel electrophoresis (SDS-PAGE) and blotted onto a polyvinylidene difluoride (PVDF) membrane. The PVDF membranes were blocked with Tris-buffered saline (TBS) containing 5% skimmed milk powder for 1 h, incubated with primary antibodies (Supplementary Table 2) overnight at 4°C. Membranes were incubated with either anti-mouse or anti-rabbit immunoglobulin G (IgG) horseradish peroxidase-conjugated secondary antibody (Amersham Biosciences, Piscataway, NJ, USA). Specific bands were visualized using ECL Western Blotting Detection Reagents (Amersham Biosciences, Piscataway, NJ, USA). The intensity of bands was quantified using Image Lab software version 2.0 (Bio-Rad Laboratories, Hercules, CA, USA), and glyceraldehyde 3-phosphate dehydrogenase (GAPDH) was used as an internal standard.

RT² profiler PCR arrays

Total RNA from 3×10^6 of T was isolated using an miRNeasy Micro Kit (Qiagen) according to the manufacturer's instructions in 3 matched MDS patients. RNA concentration and quality were evaluated by Nanodrop-ND-1000 (Celbio). cDNA was synthesized from 250 ng of total RNA using an RT² First Strand Kit (SABiosciences Corp.) following the manufacturer's instructions and used to analyze the expression levels of 84 genes (Supplementary Table 3) by RT² Profiler Human Innate & Adaptive Immune Responses PCR Array (PAHS-052Z, SABiosciences Corp.). Real-Time PCR amplification was carried out on a 7500 Real-Time PCR System (Applied Biosystems). The online tool RT² Profiler data analysis software (Qiagen) was used for data normalization and statistical analyses. The threshold cut-off point was established at >2.5-fold differential expression. The Pheatmap package was used to explore differential expression of immune genes by PCR Arrays.

Quantitative reverse-transcription polymerase chain reaction (qRT-PCR)

Total RNA was extracted from BM-MNCs of 12 matched MDS patients using the RNeasy Mini Kit (QIAGEN, Hilden, Germany) according to the manufacturer's instructions. Afterward, reverse transcription and qRT-PCR were respectively fulfilled by utilizing a Revert-AidTM First Strand cDNA Synthesis Kit (Fermentas, Burlington, ON, Canada) and SYBR Premix Ex TaqTM II (Tli RNaseH Plus) (TAKARA, Beijing, China). The threshold cycles were used to calculate relative expression levels according to the $2^{-\Delta\Delta Ct}$ method. Relative mRNA expression levels were normalized to the level of GAPDH. The primer sequences used in this investigation are shown in Supplementary Table 4.

Statistical analysis

All experiments were performed at least 3 times. Analyses of flow cytometry data were conducted using CellQuest software. Continuous variables were presented as mean \pm standard deviation (SD) or median. They were compared by a parametric (Student's t test, analysis of variance (ANOVA)) or non-parametric (Mann-Whitney U, Kruskal-Wallis) test as appropriate according to each variable distribution. Categorical variables were compared using Fisher's exact tests. Differences were considered to be statistically significant at $P < 0.05$. The statistical analyses were performed with the GraphPad Prism program (GraphPad Software, Inc., San Diego, CA, USA) or SPSS software (version 22.0).

Results

Transcriptome profiling of MDS cell lines following DAC treatment

The GEM analysis of MDS-L cell showed 1,745 differentially expressed genes compared with the control: 842 were upregulated, while 903 genes were downregulated. The GEM analysis of SKM-1 cell showed 1,303 differentially expressed genes compared with the results of the control: 541 were upregulated, while

762 genes were downregulated. The overlap among the 2 cell lines contained 256 genes. Among them, 89 genes were upregulated together and 167 genes were downregulated together.

GO terms and pathways enriched by DEGs

The GO analysis revealed that MDS cell line DEGs are involved in the process of immune-related response. BPs were mainly enriched in defense response to virus, immune response, inflammatory response, intrinsic apoptotic signaling pathway in response to DNA damage, and positive regulation of inflammatory response (Fig. 1a). For CC, enrichment of *DEGs* was mainly enriched inside the chromosome, chromosomal part, and nuclear chromosome (Fig. 1b). For MF, enrichment of *DEGs* was primarily in transcription factor binding, identical protein binding, and protein dimerization binding (Fig. 1c). KEGG pathway analysis revealed that enrichment of DEGs occurred mostly in the FOXO signaling pathway, Epstein-Barr virus infection, cellular senescence, cell cycle, and hematopoietic cell lineage (Fig. 1d). Overall, there were significantly altered transcripts participating in the FOXO signaling pathway, cell cycle, Toll-like receptor signaling pathway, hematopoietic cell differentiation, inflammatory response, and p53 signaling pathway (Fig. 1e).

Functional network of DAC-induced transcripts

The subnetwork enrichment analysis of DAC induced immune related transcripts in MDS cell lines identified TP53, FOXO1, TLR4, TLR8, S100A8, S100A9, CD14, and CXCL10 as highly interconnected genes, and are likely to be the potential hubs of the immunity functional network (Fig. 2). The FOXO1 signaling pathway containing genes AKT3, ATM, BCL2L11, BCL6, BNIP3, CAT, CCND2, CDK2, FBXO32, FOXO1, HOMER1, IL6, IL7R, KLF2, MAPK11, MAPK14, MAPK8, MAPK9, PCK1, PCK2, PIK3CD, PIK3CG, PIK3R1, PTEN, SMAD2, SMAD3, and TNFSF10 are biologically linked to numerous signal pathways, including cell apoptosis, cell cycle, cell differentiation, and immune system (Fig. 1e). In this study, we focused especially on the effect of FOXO1 on biological characteristics in MDS.

DAC Induces Apoptosis in MDS-L Cells

As DAC exposure time expanded, the percentages of apoptotic cells increased significantly (Fig. 3a). This apoptotic rate was confirmed using Annexin-V-FITC/PI double labeling, which showed a progressive increase in apoptosis on days 3 and 5, with the rate of increase in early apoptotic cells being most notable (Fig. 3b).

In the absence of DAC, the expression of activated FOXO1 was very low in MDS-L cells, but after the initiation of treatment on days 3 and 5, the expression of activated FOXO1 gradually increased, rather than the non-activated phosphorylated form (p-FOXO1). The expression of p-FOXO1 gradually decreased, indicating that FOXO1 mainly exists in an inactive form in MDS-L cells. With the prolonged action of the drug, DAC can induce FOXO1 activation in MDS-L cells (Fig. 3c). The expression of target protein downstream of apoptosis-related FOXO1 was also detected. As shown in Fig. 4C, measurable expression of apoptosis-related proteins Bim, Puma, and FasL was observed in untreated MDS-L cells. After DAC

treatment, Bim, Puma, and FasL protein expression increased significantly with the increase of exposure time to drug (Fig. 3c).

To investigate the role of FOXO1 in DAC-induced MDS-L cell apoptosis, we suppressed FOXO1 expression by targeting siRNA before DAC treatment. Western blot showed that siRNA targeting FOXO1 decreased FOXO1 expression approximately 72% compared to negative control siRNA. After DAC treatment, FOXO1 expression increased obviously in negative control siRNA-treated MDS-L cells. In contrast, there was no significant increase in FOXO1 expression when cells were treated with FOXO1-targeted siRNAs (Fig. 3d). These data confirm that FOXO1 expression is inhibited by siRNA. We also observed that FOXO1 silencing inhibited the expression of Bim that was observed following DAC treatment, but not the expression of Puma and FasL protein, suggesting that the presence and activation of FOXO1 plays a crucial role in the activation of Bim (Fig. 3d).

After knockdown of FOXO1, apoptosis assay indicated that silenced FOXO1 did not significantly affect the later apoptosis of MDS-L cells, but significantly decreased early apoptosis of MDS-L cells, suggesting that FOXO 1 activation is involved mostly in the early stages of DAC-induced apoptosis (Fig. 3e).

DAC Induces Cell Cycle Arrest in MDS-L Cells

After DAC treatment, the proportion of cells in S phase decreased significantly, while the proportion of cells in G0/G1 phase increased, indicating that cell cycle arrest was induced by G0/G1 blockade (Fig. 4a, b).

The impact of DAC treatment on cell cycle gene expression was also observed. CDKN1A, CDKN1B, CCND1, and CCND2 are downstream genes targeted by FOXO1 and are disordered in a variety of tumors. As shown in Fig. 4C, the expression of CDKN1A and CDKN1B was rare in untreated MDS-L cells, but after DAC treatment, the expression of CDKN1A and CDKN1B was upregulated with drug maintenance application. Conversely, a significant decrease in CCND1 and CCND2 expression was observed in the presence of DAC (Fig. 4c).

Then, we studied the effect of silent FOXO1 on CDKN1A, CDKN1B, CCND1, and CCND2. Compared with control siRNA, silencing FOXO1 had significant effects on the cell cycle. The expression of FOXO1 downstream targets CDKN1A, CCND1, and CCND2 were obviously affected, whereas silencing FOXO1 had no significant effect on CDKN1B (Fig. 4d). In the presence of FOXO1 silencing, DAC showed no ability to regulate either CDKN1B protein expression, indicating FOXO1 has a regulatory effect to CDKN1A, CCND1 and CCND2 (Fig. 4d).

The increase in the proportion of S phase cells in MDS-L following knockdown of FOXO1 was not totally reversed by subsequent DAC treatment, suggesting that FOXO1 activation plays an indispensable role in DAC-induced cell cycle arrest (Fig. 4e).

FOXO1 Contributes to DAC-Induced MDS-L Cell Differentiation

MDS-L cells were positive for CD34, c-Kit, HLA-DR, CD13, and CD33 and partially positive for CD41 and negative for CD3, CD14, CD20, and CD235a [21]. The expression levels of myeloid cell antigen CD13, T lymphocyte cell marker CD3, monocyte differentiation marker CD14, B lymphocyte differentiation marker CD20, and erythroid cell differentiation marker CD235a on the surface of DAC treated MDS-L cells were detected. The expression levels of CD3, CD14, and CD20 on the surface of MDS-L cells increased after DAC treatment, accompanied by antigen changes, with CD13 showing a significant decrease after treatment (Fig. 5a, b), while the expression of CD235a showed no obvious change during DAC treatment. As DAC action time was prolonged, the expression levels of CD3, CD14, and CD20 continued to increase in a time-dependent manner (Fig. 5a, b).

No significant difference in cell differentiation antigen expression was observed between MDS-L cells in which FOXO1 was silenced and non-silenced control. However, when FOXO1 siRNA-MDS-L cells were treated with DAC, the observed increase in CD3-positive cells were significantly reduced compared to cells carrying negative control siRNA (Fig. 5c), indicating that silencing FOXO1 before DAC treatment weakens, but does not eliminate the differentiation of DAC-induced MDS-L cells into antigen molecules. Therefore, the above studies indicate that FOXO1 activation contributes to DAC-induced MDS cell differentiation.

FOXO1 Contributes to DAC-Mediated TLR-4 Augment in MDS-L Cells

The PTEN/PI3K/AKT/FOXO1 signaling pathway is a major signaling pathway involved in cell proliferation, apoptosis, metastasis, and immunoregulation, and its cascade reaction pathway occupies an important position in the signal transduction process [22]. In the present study, the protein expression of PTEN, FOXO1, p-PI3K, p-AKT, and TLR-4 was also detected employing western blot. The results showed that the protein expression of PTEN, FOXO1, and TLR-4 increased after DAC treatment, accompanied by significant decreases in p-PI3K, and p-AKT (Fig. 5d). Compared with the negative control group, FOXO1 siRNA-MDS-L cells treated with DAC, the expression of PTEN showed significant upregulation, but the expression of FOXO1 and TLR-4 showed a significant decrease (Fig. 5e). Thus, DAC induces PTEN, which in turn activates FOXO1 signaling, leading to the activation TLR4-driven innate immune response.

FOXO1 Contributes to DAC-Mediated Immune Activation in MDS Patients

Because MDS-L lacks innate and adaptive immune cells, MDS patient specimens were used to verify the effect of FOXO1 on innate and adaptive immunity in vivo. The transcriptional profiling of 84 genes involving innate and adaptive immune processes were evaluated after 4 courses DAC treatment in 3 matched MDS patients (n = 3) (Supplementary Table 1). The transcriptional profiling analysis was performed on isolated T cells. A total of 37 (44%) genes were differentially expressed after DAC treatment with fold changes >2.5 (Fig. 6a). Among these, a total of 23 (27.4%) innate and adaptive immunity genes were significantly upregulated. The altered transcriptional profiling of MDS T cells was characterized by the upregulation of innate and adaptive immunity genes. Meanwhile, the expression of FOXO1, STAT1, T-bet, PD-1, and PD-L1 was also detected in 12 paired MDS patients by RT-PCR due to the limiting amount

of the panel. As shown in Fig. 6b, the mRNA level of FOXO1, T-bet, STAT1, PD-1, and PD-L1 was highly upregulated after 4 courses of DAC treatment. Furthermore, the protein expression level of FOXO1, p-FOXO1, p-STAT3, and T-bet was detected by western blot in 1 MDS patient. As shown in Fig. 6c, the expression of activated FOXO1, p-STAT1, p-STAT3, and T-bet increased, while the expression of non-activated p-FOXO1 reduced after DAC treatment. Therefore, the above studies demonstrate that FOXO1 activation contributes to DAC-induced immune activation in MDS.

Discussion

MDS represents a preleukemic state of ineffective hematopoiesis hallmarked by bone marrow dysplasia that easily progresses into acute myeloid leukemia [23]. For higher-risk MDS patients who are not suitable for transplant, HMAs are most appropriate. DAC are therapeutic agents and have already been used in treatment of higher-risk MDS and acute myeloid leukemia for many years. DAC can play a role in decreasing MDS clonal burden and may therefore resulting in improved hematopoiesis, but do not eradicating transformed stem cells, so relapse is inevitable. The mechanism of action of DAC is still not fully understood, and may result from a combination of conventional cytotoxic, DNA hypomethylation and immune-related mechanisms including changes in interferon signaling and presentation of neoantigens as epitopes to the immune system [6, 24, 25]. Once DAC fails the patient, either via intolerance, resistance, or relapse after favorable response, there is limited approved second-line therapy and the outlook is poor with a median survival of less than 6 months [26–28]. Therefore, clarifying the mechanism underlying DAC is required to improve the treatment effect in MDS.

DAC is considered a quick and profound global DNA demethylation, as well as site-specific promoter demethylation of many genes including cancer suppressor genes and immune-related genes [29, 30]. In this study, using the DEG analytical method, the data suggest that multiple genes and multigenic pathways were regulated by DAC. For example, DAC could activate the interferon signaling and p53 signaling pathway induce further biological process in pathway analysis as previous reports [4–6]. However, this study focused on the mechanism of tumor suppressor gene FOXO1 in decitabine-dependent processes. The results showed that FOXO1 is hyperphosphorylated and thus inactivated in MDS-L cells. DAC treatment activated FOXO1 by both increasing expression and reducing phosphorylation, leading to the upregulation of the downstream effectors Bim, Puma, FasL, CDKN1A, and CDKN1B and the downregulation of the downstream cell cycle effectors Cyclin D1 and Cyclin D2. Furthermore, DAC-induced differentiation of MDS-L cells into lymphocytes and monocytes, MDS-L cell cycle arrest, apoptosis, and immune activation were also observed.

Forkhead box O (FOXO) transcription factors, including FOXO1 (FKHR), FOXO3a (FKHRL1), FOXO4 (AFX), and FOXO6, have also been increasingly recognized as tumor suppressors through serving as key connection points to allow diverse, proliferative nutrient and stress signals to converge and integrate with distinct gene networks to control cell fate, metabolism, and cancer development [31, 32]. As shown in Fig. 6d, FOXO1 expression is reduced in most tumors and appears to act as a tumor suppressor gene. In this study, similar to the effect of FOXO3A activation in the SKM-1 cell line [9], active FOXO1 also plays an

important role in suppressing MDS-L by inducing apoptosis and by inhibiting cell cycle progression. In contrast to active FOXO3A, our research confirmed that activated FOXO1 tends to directly regulate Bim gene, which is consistent with previous research [33, 34]. That is, activated FOXO1 is translocated to the nucleus, binding to the Bim promoter and induces the transcription of the Bim gene. However, FOXO1 activation showed a limited regulation effect on Puma and FasL expression by silencing FOXO1, which shows that DAC may up-regulate the expression of Puma and FasL in other ways. It is therefore likely that the apoptosis induced by DAC was mediated primarily through the mitochondrial apoptosis pathway. Through a similar silencing FOXO1 gene function test, we also found that FOXO1 has a more closely regulatory effect on CDKN1A, CCND1, and CCND2 than on CCND1 [35].

Next, we focused on the role of FOXO1 in the MDS immune microenvironment. As shown in Fig. 6e, FOXO1 also intrinsically controls the anti-tumor immune response as well as the homeostasis and development of immune cells, including T cells, B cells, natural killer (NK) cells, macrophages, and dendritic cells. However, the mechanism of FOXO1 in the MDS immune environment has not been reported so far. In the past decade, aberrant immune activation in lower risk MDS and impaired anti-leukemic immunity in higher risk MDS within the malignant clone and the bone marrow microenvironment were identified as key pathogenic drivers of MDS. Multiple mechanisms are involved in higher risk MDS to promote immune tolerance [36, 37]. Several reports have demonstrated that higher risk disease is accompanied by an increase in myeloid-derived suppressor cells (MDSCs), along with regulatory T cells (Tregs) augmentation [38, 39]. One effect of increasing suppressive cell subsets is reduction of cytotoxic anti-leukemia immunity. The activation and function of natural killer (NK) cells and cytotoxic T lymphocytes (CTL) exert important cytotoxic activity in response to myeloid neoplasms, but their function is reduced in high-risk MDS [40, 41]. In our study, we found that DAC promotes the differentiation of MDS-L cell surface antigen into lymphocytes and monocytes through activating FOXO1. Further PTEN/PI3K/AKT/FOXO1 pathway study confirmed that DAC upregulates PTEN gene expression, thereby inhibiting the phosphorylation of PI3K and AKT and releasing FOXO1 inhibition. Activated FOXO1 can upregulate TLR4 expression, thereby activating the MDS innate immune system. The results were consistent with previous studies, FOXO1 is a key regulator of many inflammatory factors, such as TLR4, NF- κ B, tumor necrosis factor (TNF)- α , interleukin (IL)-1 β , and IL-18, via the TLR4/NF- κ B signaling pathway [42, 43]. In the specimens of MDS patients, we further verified that with the increased expression of FOXO1, there is a wide range of upregulation and activation of type I immune cell transcription factors and up-regulation of cellular immune functions, thereby enhancing anti-leukemia effects and inhibiting the growth of MDS malignant clones. All the results demonstrated that DAC can activate FOXO1 to enhance anti-tumor immune effect in higher risk MDS.

Accumulating evidence has shown the paradoxical intrinsic role of the FOXO1 in cancer, which can act as a tumor repressor while also maintaining cancer stem cells [44, 45]. The regulatory role of FOXO1 in tumor immunity is equally confusing [46]. DAC also has a double-edged sword effect on the regulation of MDS immune function. The global demethylation of DNA can induce anti-tumor effects. It can also upregulate the expression of inhibitory immune checkpoint receptors and their ligands, resulting in secondary resistance to DAC [47]. Due to the limitation of conditions, we do not have an appropriate MDS

animal model to further verify activated FOXO1 in cancer cells, stromal cells, and immune cells, along with their extracellular factors, which have profound effects on either promoting or repressing anticancer immunity in the tumor microenvironment (TME). The effect of activated FOXO1 on the prognosis and survival of MDS disease also requires further long-term follow-up. Based on the above findings, we agree with assumption of Wolff F, who proposed a role for FOXO1 as a rheostat, regulating both immune homeostasis and the immune response in cancer immunity. In the future, further study is needed to better understand the role of FOXO1 in MDS pathogenesis. It will be interesting to gain a better understanding of each molecule and each cell type that is regulated by FOXO1 directly in the setting of cancer patients or tumor models [48].

Conclusions

In conclusion, this study showed that silencing FOXO1 expression impaired DAC-induced apoptosis, cell cycle arrest, and cellular differentiation, potentially because of the observed downregulation of Bim, CDKN1A, CCND1, and CCND2. DAC-induced TLR4 upregulation was mainly reversed by FOXO1 silencing, which could explain the partial reversal of DAC-induced immune activation that is observed when FOXO1 expression is knocked down. The upregulation of the innate and adaptive immunity genes following DAC treatment, as well as the consequent increase in T-bet, p-FOXO1 and p-STAT3 in MDS specimen, was found to be related to the DAC-induced upregulation and activation of FOXO1. Collectively, DAC induces FOXO1 activation, which plays an important role in anti-MDS tumors.

Abbreviations

MDS: myelodysplastic syndromes; DAC: decitabine; DEGs: differential expressed genes; GO: gene ontology; KEGG: Kyoto Encyclopedia of Genes and Genomes; IPSS: International Prognostic Scoring System; HMAs: hypomethylating agents; CTAs: cancer-testis antigens; GEM: gene expression microarray; BP: biological process; CC: cellular component; MF: molecular function; PPI: protein–protein interaction network; MCODE: molecular complex detection; WHO: World Health Organization; BM-MNCs: bone marrow mononuclear cells.

Declarations

Authors' contributions

Zheng Zhang analyzed and interpreted the principal data regarding cell functional analysis and western blotting. Yan Jia, Feng Xv, Lu-xi Song, Lei Shi, and Juan Guo were involved in the in vivo experiments and the statistical analysis. Chun-kang Chang was responsible for the design of the study and drafting the manuscript. All authors have read and approved the final version of the manuscript.

Author details

¹Dept. of Hematology, Shanghai Jiao Tong University Affiliated Sixth People's Hospital, No. 600 Yishan Road, Shanghai, 200233, China.

Acknowledgements

Not applicable.

Competing interests

The authors declare that they have no competing interests.

Available of data and materials

The datasets used and/or analyzed during the present study are available from the corresponding author upon reasonable request.

Consent for publication

Not applicable.

Ethics approval and consent to participate

All experiments were performed in compliance with relevant laws and guidelines. All experiments were conducted following the institutional guidelines of the ethics committee of Shanghai Jiao Tong University Affiliated Sixth People's Hospital.

Funding

This study was supported by the National Natural Science Foundation of China (Grant No. 81400091, 81770121).

References

1. Zeidan AM, Shallis RM, Wang R, et al. Epidemiology of myelodysplastic syndromes: Why characterizing the beast is a prerequisite to taming it. *Blood Rev.* 2019; 34:1-15. <https://doi.org/10.1016/j.blre.2018.09.001>.
2. Greenberg P, Cox C, LeBeau MM, et al. International scoring system for evaluating prognosis in myelodysplastic syndromes. *Blood.* 1997;89(6):2079-88.
3. Greenberg PL, Tuechler H, Schanz J, et al. Revised international prognostic scoring system for myelodysplastic syndromes. *Blood.* 2012;120(12):2454-65. <https://doi.org/10.1182/blood-2012-03-420489>.
4. Chang CK, Zhao YS, Xu F, et al. TP53 mutations predict decitabine-induced complete responses in patients with myelodysplastic syndromes. *Br J Haematol.* 2017;176(4):600-608. <https://doi.org/10.1111/bjh.14455>.

5. Zhang Z, Chang CK, He Q, et al. Increased PD-1/STAT1 ratio may account for the survival benefit in decitabine therapy for lower risk myelodysplastic syndrome. *Leuk Lymphoma*. 2017;58(4):969-978. <https://doi.org/10.1080/10428194>.
6. Zhang Z, He Q, Tao Y, et al. Decitabine treatment sensitizes tumor cells to T-cell-mediated cytotoxicity in patients with myelodysplastic syndromes. *Am J Transl Res*. 2017;9(2):454-465.
7. Itzykson R, Fenaux P. Epigenetics of myelodysplastic syndromes. *Leukemia*. 2014;28(3):497-506. <https://doi.org/10.1038/leu.2013.343>.
8. Link W, Fernandez-Marcos PJ. FOXO transcription factors at the interface of metabolism and cancer. *Int J Cancer*. 2017;141(12):2379-2391. <https://doi.org/10.1002/ijc.30840>.
9. Zeng W, Dai H, Yan M, et al. Decitabine-Induced Changes in Human Myelodysplastic Syndrome Cell Line SKM-1 Are Mediated by FOXO3A Activation. *J Immunol Res*. 2017; 2017:4302320. <https://doi.org/10.1155/2017/4302320>.
10. Murtaza G, Khan AK, Rashid R, et al. FOXO Transcriptional Factors and Long-Term Living. *Oxid Med Cell Longev*. 2017;2017:3494289. <https://doi.org/10.1155/2017/3494289>.
11. Jiang S, Li T, Yang Z, et al. Deciphering the roles of FOXO1 in human neoplasms. *Int J Cancer*. 2018;143(7):1560-1568. <https://doi.org/10.1002/ijc.31338>.
12. Chen J, Lu Y, Tian M, et al. Molecular mechanisms of FOXO1 in adipocyte differentiation. *J Mol Endocrinol*. 2019;62(3): R239-R253. <https://doi.org/10.1530/JME-18-0178>.
13. Xing YQ, Li A, Yang Y, et al. The regulation of FOXO1 and its role in disease progression. *Life Sci*. 2018; 193:124-131. <https://doi.org/10.1016/j.lfs.2017.11.030>.
14. Brownawell AM, Kops GJ, Macara IG, et al. Inhibition of nuclear import by protein kinase B (Akt) regulates the subcellular distribution and activity of the forkhead transcription factor AFX. *Mol Cell Biol*. 2001; 21(10):3534-46. <https://doi.org/10.1128/MCB.21.10.3534-3546.2001>.
15. Ushmorov A, Wirth T. FOXO in B-cell lymphopoiesis and B cell neoplasia. *Semin Cancer Biol*. 2018; 50:132-141. <https://doi.org/10.1016/j.semcancer.2017.07.008>.
16. Shi F, Li T, Liu Z, et al. FOXO1: Another avenue for treating digestive malignancy? *Semin Cancer Biol*. 2018; 50:124-131. <https://doi.org/10.1016/j.semcancer.2017.09.009>.
17. Tohyama K, Tohyama Y, Nakayama T, et al. A novel factor-dependent human myelodysplastic cell line, MDS92, contains haemopoietic cells of several lineages. *Br J Haematol*; 91(4):795-9. <https://doi.org/10.1111/j.1365-2141.1995.tb05391.x>.
18. Nakagawa T, Matozaki S. The SKM-1 leukemic cell line established from a patient with progression to myelomonocytic leukemia in myelodysplastic syndrome (MDS)-contribution to better understanding of MDS. *Leuk Lymphoma*. 1995;17(3-4):335-9. <https://doi.org/10.3109/10428199509056841>.
19. Xu F, He Q, Li X, et al. Rigosertib as a selective anti-tumor agent can ameliorate multiple dysregulated signaling transduction pathways in high-grade myelodysplastic syndrome. *Sci Rep*. 2014; 4:7310. <https://doi.org/10.1038/srep07310>.

20. Arber DA, Orazi A, Hasserjian R, et al. The 2016 revision to the World Health Organization Classification of myeloid neoplasms and acute leukemia. *Blood*. 2016;127(20):2391-405. <https://doi.org/10.1182/blood-2016-03-643544>.
21. K Tohyama, H Tsutani, T Ueda, et al. Establishment and characterization of a novel myeloid cell line from the bone marrow of a patient with the myelodysplastic syndrome. *Br J Haematol*. 1994;87(2):235-42. <https://doi.org/10.1111/j.1365-2141.1994.tb04904.x>.
22. Jiang S, Li T, Yang Z, et al. Deciphering the roles of FOXO1 in human neoplasms. *Int J Cancer*. 2018;143(7):1560-1568. <https://doi.org/10.1002/ijc.31338>.
23. Steensma DP. Myelodysplastic syndromes current treatment algorithm 2018. *Blood Cancer J*. 2018;8(5):47. <https://doi.org/10.1038/s41408-018-0085-4>.
24. Licht, J. D. DNA methylation inhibitors in cancer therapy: the immunity dimension. *Cell*. 2015;162(5):938-9. <https://doi.org/10.1016/j.cell.2015.08.005>.
25. Chiappinelli KB, Strissel PL, Desrichard A, et al. Inhibiting DNA Methylation causes an interferon response in cancer via dsRNA including endogenous retroviruses. *Cell*. 2017;169(2):361. <https://doi.org/10.1016/j.cell.2017.03.036>.
26. Montalban-Bravo G, Garcia-Manero G, Jabbour E. Therapeutic choices after hypomethylating agent resistance for myelodysplastic syndromes. *Curr Opin Hematol*. 2018;25(2):146-153. <https://doi.org/10.1097/MOH.0000000000000400>.
27. **Prébet T, Gore SD, Esterni B**, et al. Outcome of high-risk myelodysplastic syndrome after azacytidine treatment failure. *J Clin Oncol*. 2011;29(24):3322-7. <https://doi.org/10.1200/JCO.2011.35.8135>.
28. Jabbour E, Garcia-Manero G, Batty N, et al. Outcome of patients with myelodysplastic syndrome after failure of decitabine therapy. 2010;116(16):3830-4. <https://doi.org/10.1002/cncr.25247>.
29. Wolff F, Leisch M, Greil R, et al. The double-edged sword of (re)expression of genes by hypomethylating agents: from viral mimicry to exploitation as priming agents for targeted immune checkpoint modulation. *Cell Commun Signal*. 2017;15(1):13. <https://doi.org/10.1186/s12964-017-0168-z>.
30. Seelan RS, Mukhopadhyay P, Pisano MM, et al. Effects of 5-Aza-2'-deoxycytidine (decitabine) on gene expression. *Drug Metab Rev*. 2018;50(2):193-207. <https://doi.org/10.1080/03602532.2018.1437446>.
31. Jiramongkol Y, Lam EW. FOXO transcription factor family in cancer and metastasis. *Cancer Metastasis Rev*. 2020. <https://doi.org/10.1007/s10555-020-09883-w>.
32. **Farhan M, Wang H, Gaur U**, et al. FOXO Signaling Pathways as Therapeutic Targets in Cancer. *Int J Biol Sci*. 2017;13(7):815-827. <https://doi.org/10.7150/ijbs.20052>.
33. Dijkers PF, Medema RH, Lammers JW, et al. Expression of the pro-apoptotic Bcl-2 family member Bim is regulated by the forkhead transcription factor FKHR-L1. *Curr Biol*. 2000;10(19):1201-4. [https://doi.org/10.1016/s0960-9822\(00\)00728-4](https://doi.org/10.1016/s0960-9822(00)00728-4).
34. Dijkers PF, Birkenkamp KU, Lam EW, et al. FKHR-L1 can act as a critical effector of cell death induced by cytokine withdrawal: protein kinase B-enhanced cell survival through maintenance of

- mitochondrial integrity. *J Cell Biol.* 2002;156(3):531-42. <https://doi.org/10.1083/jcb.200108084>.
35. Schmidt M, Fernandez de Mattos S, van der Horst A, et al. Cell cycle inhibition by FoxO forkhead transcription factors involves downregulation of cyclin D. *Mol Cell Biol.* 2002;22(22):7842-52. <https://doi.org/10.1128/mcb.22.22.7842-7852.2002>
36. Sallman DA, List A. The central role of inflammatory signaling in the pathogenesis of myelodysplastic syndromes. 2019;133(10):1039-1048. <https://doi.org/10.1182/blood-2018-10-844654>.
37. Ivy KS, Brent Ferrell P Jr. Disordered Immune Regulation and its Therapeutic Targeting in Myelodysplastic Syndromes. *Curr Hematol Malig Rep.* 2018;13(4):244-255. <https://doi.org/10.1007/s11899-018-0463-9>.
38. Gabilovich DI, Nagaraj S. Myeloid-derived suppressor cells as regulators of the immune system. *Nat Rev Immunol.* 2009;9(3):162–74. <https://doi.org/10.1038/nri2506>.
39. Kittang AO, Kordasti S, Sand KE, et al. Expansion of myeloid derived suppressor cells correlates with number of T regulatory cells and disease progression in myelodysplastic syndrome. *Oncoimmunology.*2016;5(2): e1062208. <https://doi.org/10.1080/2162402x.2015.1062208>.
40. Epling-Burnette PK, Bai F, Painter JS, et al. Reduced natural killer (NK) function associated with high-risk myelodysplastic syndrome (MDS) and reduced expression of activating NK receptors. *Blood.* 2007;109(11):4816–24. <https://doi.org/10.1182/blood-2006-07-035519>.
41. Kotsianidis I, Bouchliou I, Nakou E, et al. Kinetics, function and bone marrow trafficking of CD4+CD25+FOXP3+ regulatory T cells in myelodysplastic syndromes (MDS). *Leukemia.* 2009;23(3):510-8. <https://doi.org/10.1038/leu.2008.333>.
42. Li Z, He Q, Zhai X, et al. Foxo1-mediated inflammatory response after cerebral hemorrhage in rats. *Neurosci Lett.* 2016; 629:131-136. <https://doi.org/10.1016/j.neulet.2016.06.013>.
43. Kamo N, Ke B, Busuttill RW, et al. PTEN-mediated Akt/ β -catenin/Foxo1 signaling regulates innate immune responses in mouse liver ischemia/reperfusion injury. 2013; 57(1):289-98. <https://doi.org/10.1002/hep.25958>.
44. Sykes SM, Lane SW, Bullinger L, et al. AKT/FOXO signaling enforces reversible differentiation blockade in myeloid leukemias. 2011;146(5):697-708. <https://doi.org/10.1016/j.cell.2011.07.032>.
45. Long J, Jia MY, Fang WY, et al. FLT3 inhibition upregulates HDAC8 via FOXO to inactivate p53 and promote maintenance of FLT3-ITD+ acute myeloid leukemia. 2020;135(17):1472-1483. <https://doi.org/10.1182/blood.2019003538>.
46. Deng Y, Wang F, Hughes T, et al. FOXOs in cancer immunity: Knowns and unknowns. *Semin Cancer Biol.* 2018; 50:53-64. <https://doi.org/10.1016/j.semcancer.2018.01.005>.
47. Wolff F, Leisch M, Greil R, et al. The double-edged sword of (re)expression of genes by hypomethylating agents: from viral mimicry to exploitation as priming agents for targeted immune checkpoint modulation. *Cell Commun Signal.* 2017;15(1):13. <https://doi.org/10.1186/s12964-017-0168-z>.

Figures

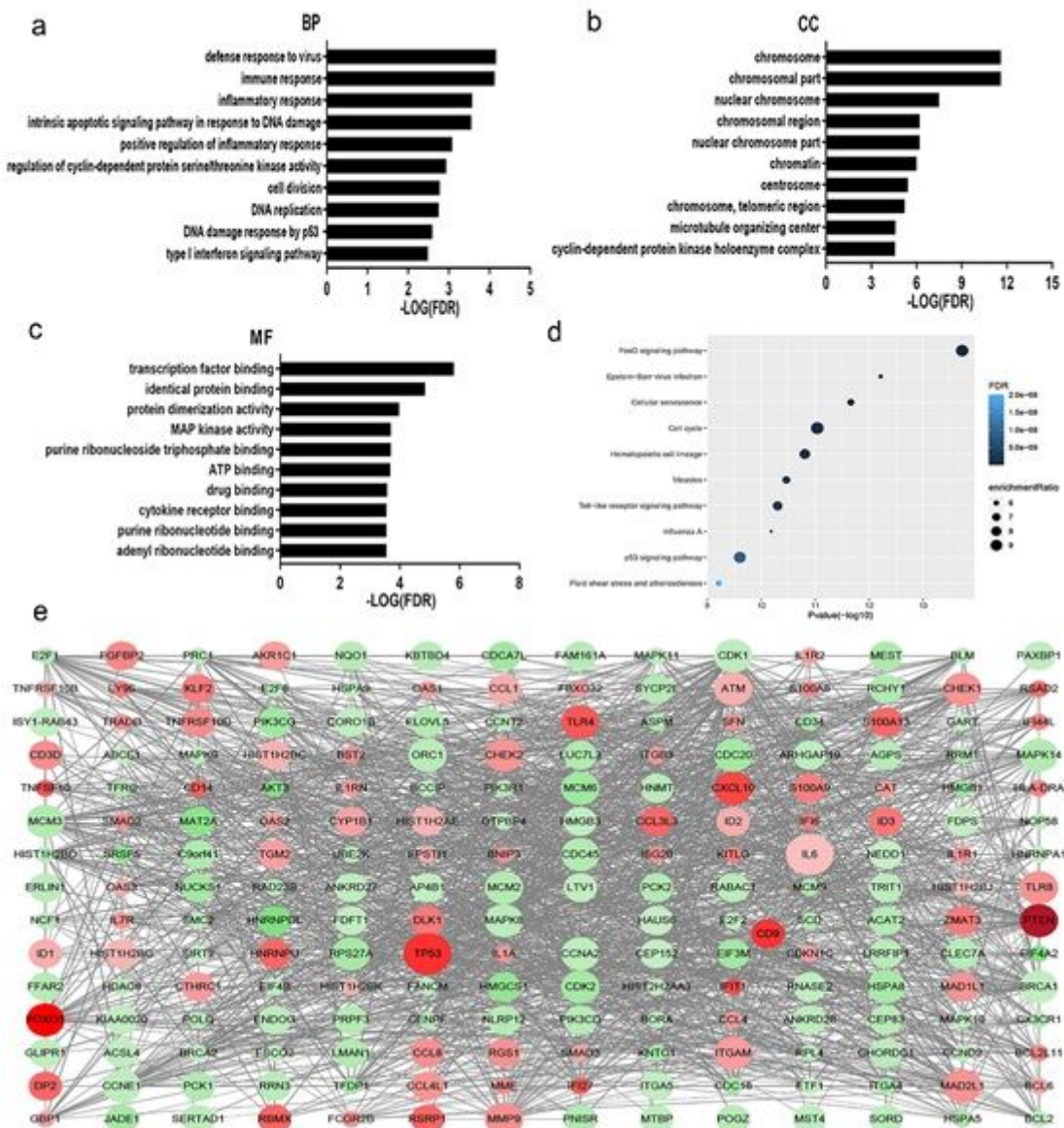


Figure 1

GO analysis and KEGG analysis. a biological process (BP), b cellular component (CC) and c molecular function (MF) in GO analysis revealed the relationship between hub genes and functional pathways. d Top 10 pathway enrichment was shown by bubble chart in KEGG analysis. The FDR=0.05 was considered as significance. e A DEG PPI network was constructed, containing 256 DEGs based on the STRING online database (89 upregulated DEGs labeled in red and 167 downregulated DEGs labeled in green). The size of dots represents the node degree.

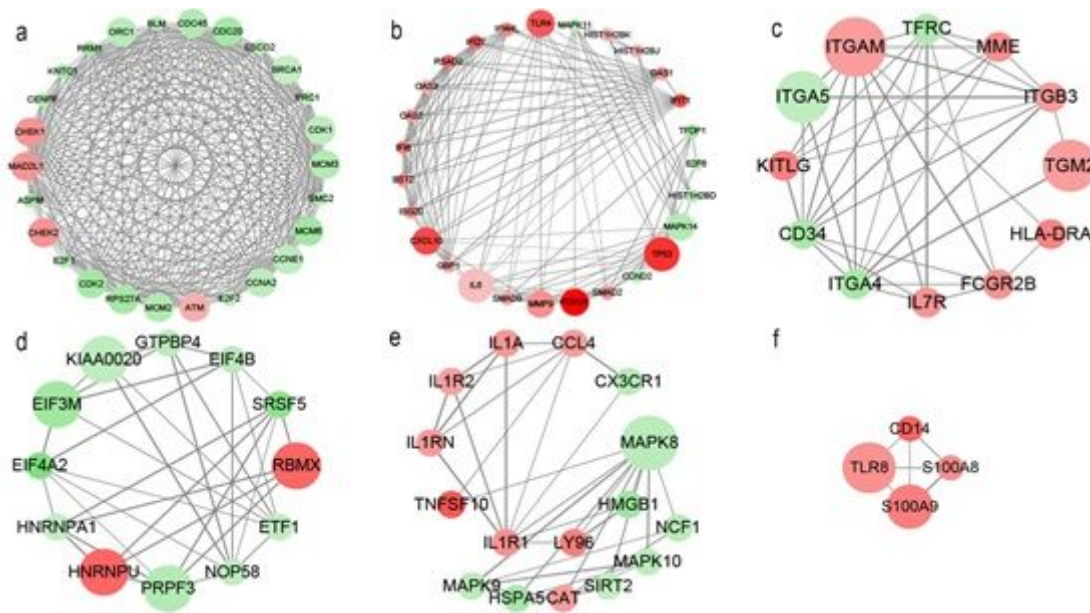


Figure 2

MCODE analysis. MCODE analysis was based on the degree of importance, and 6 main subnetworks were displayed. Upregulated genes are marked in red; downregulated genes are marked in green. The size of dots represents the node degree.

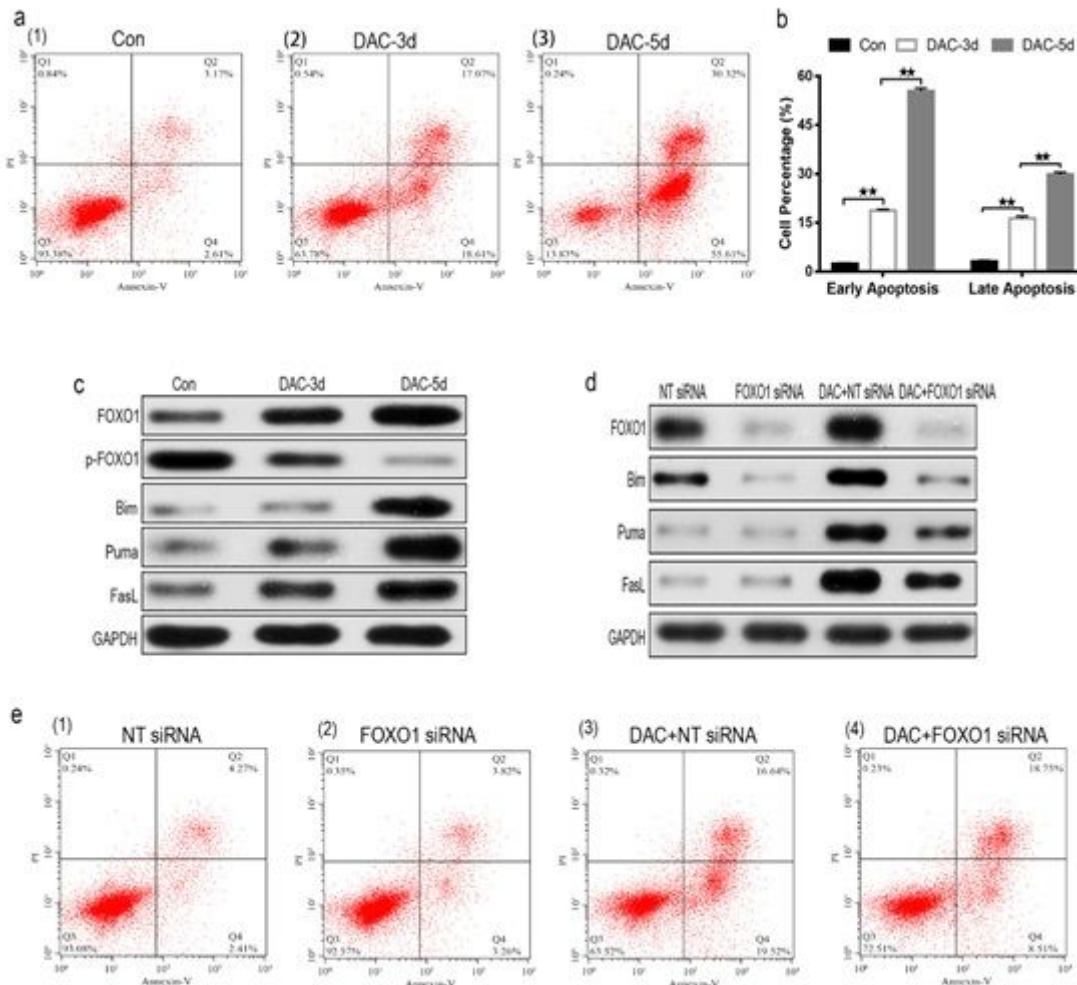


Figure 3

DAC induces apoptosis in MDS-L cells. a Annexin-V-FITC/PI assay showed that apoptosis occurred in MDS-L cells with DAC prolonged exposure time. b FCM assay detected that DAC treatment could induce both early and late apoptosis in MDS-L cells. c Western blot found that FOXO1, Bim, Puma, and FasL in MDS-L cells increased with p-FOXO1 protein, decreasing after DAC treatment. d FOXO1 silencing had no obvious influence on Puma and FasL but decreased the expression of Bim that was observed following DAC treatment. e MDS-L cell early apoptosis was partly inhibited after FOXO1 silencing and could not be significantly induced by subsequent DAC treatment. \square Student's t-test $P < 0.01$ and \square $P < 0.05$.

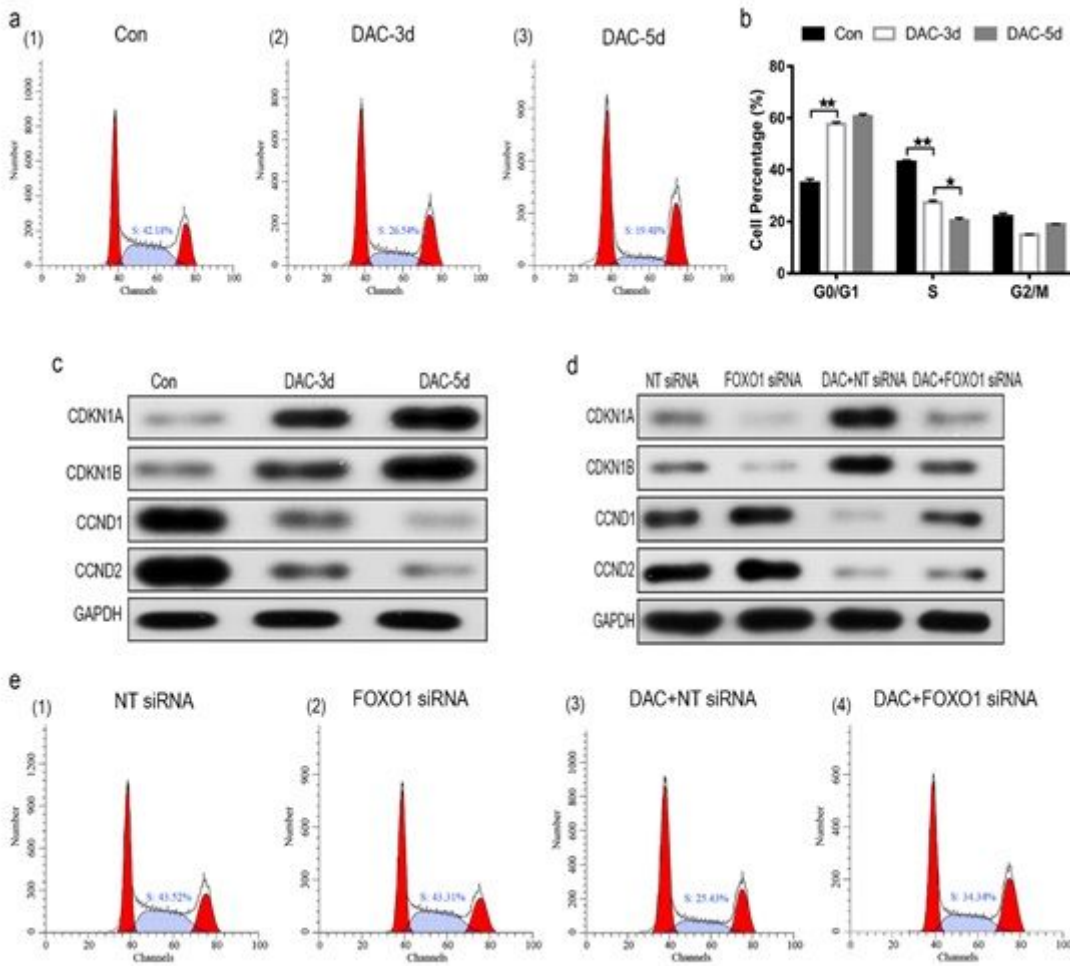


Figure 4

DAC induces cell cycle arrest in MDS-L cells. a, b Annexin-V-FITC/PI assay showed that DAC treatment could decrease cells in S phase and arrest MDS-L cells in G0/G1 and G2/M phases. c Western blot found that CDKN1A and CDKN1B in MDS-L cells increased with CCND1 and CCND2 protein decreasing after DAC treatment. d FOXO1 silencing had no obvious influence on CDKN1B and CCND1 but decreased the expression of CDKN1A and CCND2 that was observed following DAC treatment. e DAC-induced reduction of MDS-L cells in the S phase was significantly attenuated after silencing FOXO1. \square Student's t-test $P < 0.01$ and \square $P < 0.05$.

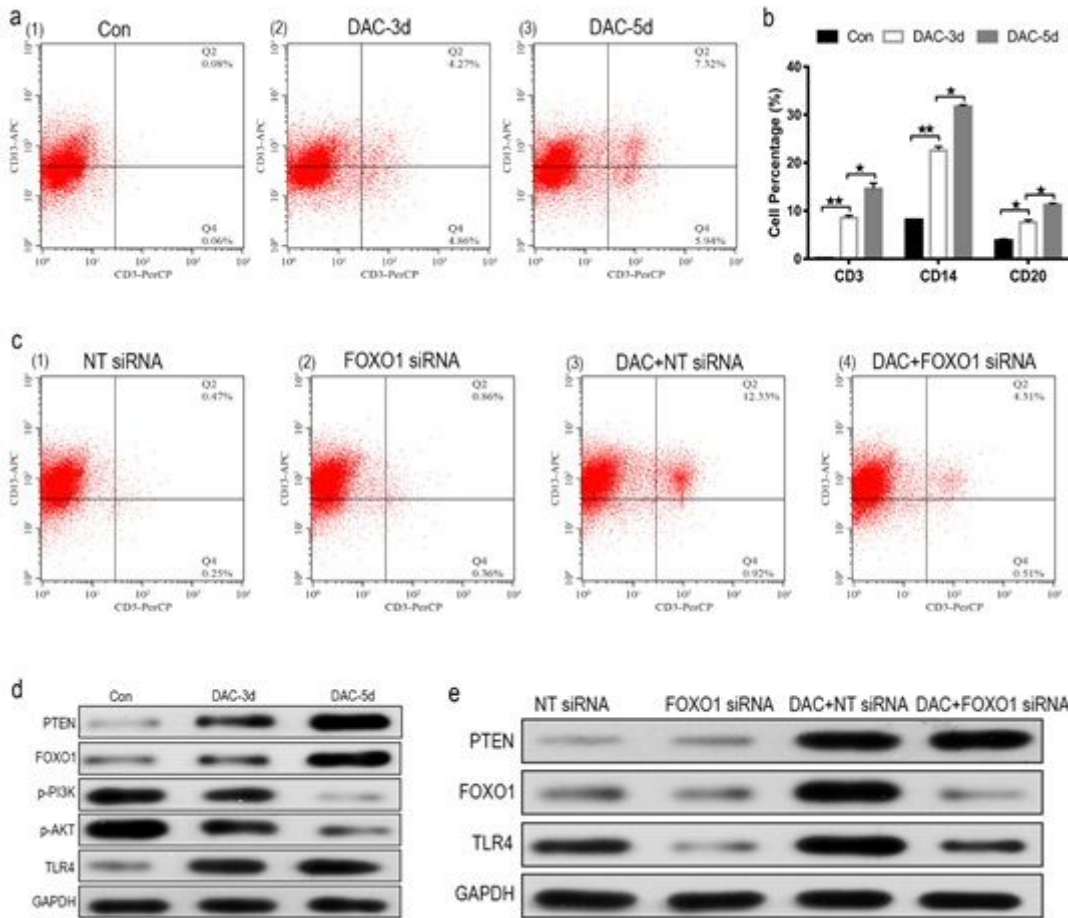


Figure 5

FOXO1 contributes to DAC-induced MDS-L cell differentiation. a CD3 expression on CD13 was significantly induced in MDS-L cells treated with DAC for different action times. b The percentage of CD13 expressing CD3, CD14, and CD20 antigen increased following DAC treatment. c Surface CD3 and CD13 expression had clearly no change between FOXO1 siRNA and negative control siRNA in MDS-L cells, while surface CD3 expression was impaired in FOXO1 siRNA compared with negative control siRNA in DAC-treated MDS-L cells. d Western blot showed that PTEN, FOXO1, and TLR4 in MDS-L cells increased with p-PI3K and p-AKT protein decreasing after DAC treatment. e FOXO1 silencing had no obvious influence on PTEN but decreased the expression of TLR4 that was observed following DAC treatment. \square Student's t-test $P < 0.01$ and \square $P < 0.05$.

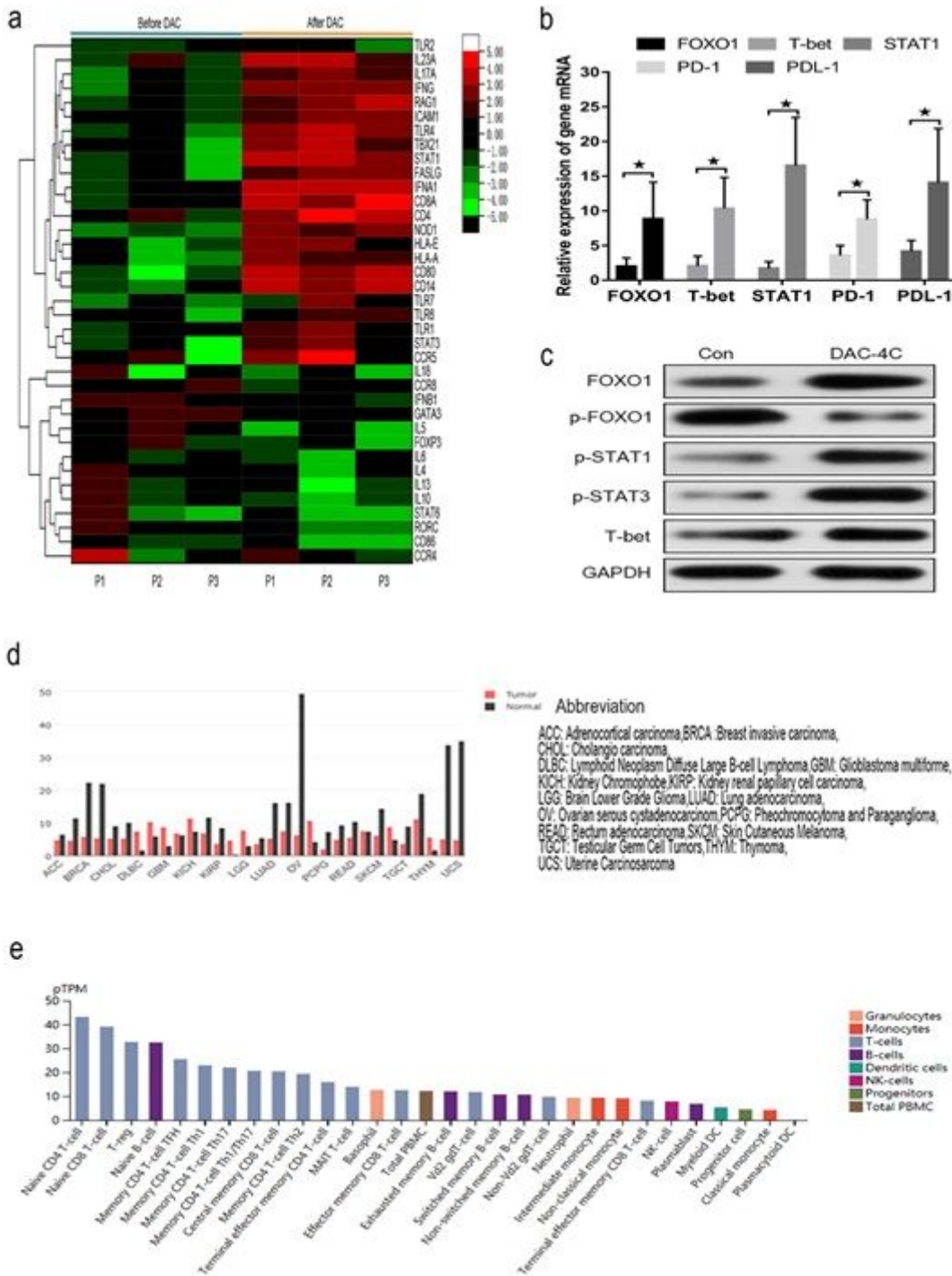


Figure 6

a Hierarchical heat map showing the DEGs in immune processes after DAC treatment. Normalized log₂ transformed values as determined by RT2 Profiler Human Innate & Adaptive Immune Responses PCR Array in T lymphocytes of 3 matched MDS patients collected at non-DAC and 4-course-DAC treatment. Each column represents 1 MDS patient, and each horizontal line refers to 1 gene. The cutoff value of log fold change as >1.5 or <-1.5, and false discovery rate <0.01 was considered. b The bar charts showed that expression of FOXO1, T-bet, STAT1, PD-1, and PDL-1 increased significantly after DAC treatment. c

Western blot showed that FOXO1, p-STAT1, p-STAT3, and T-bet in 1 MDS patient increased with p- FOXO1 protein decreasing after DAC treatment. d Using the GEPIA (Gene Expression Profiling Interactive Analysis) dataset (<http://gepia.cancer-pku.cn/>), we compared the mRNA expression of FOXO1 between different tumors and normal tissues. The results indicated that the expression levels of FOXO1 were higher in normal tissues than in tumors. The gene expression profile across different tumor samples and paired normal tissues (Bar plot). The height of bar represents the median expression of certain tumor type or normal tissue. e Utilizing an online tool (The Human Protein Atlas which aim to map all the human proteins in cells, tissues and organs using integration of various omics technologies, <https://www.proteinatlas.org/>), we explored the mRNA expression of FOXO1 in immune cells. The results show that FOXO1 plays an important role in immune cell development. Student's t-test $P < 0.05$.

Supplementary Files

This is a list of supplementary files associated with this preprint. Click to download.

- [Supplementary.docx](#)